REPORT DOCUMENTATION PAGE

Form Approved OMB NO. 0704-0188

1. REPORT DATE (DD-MM-YYYY)	2. REPORT TYPE	3. DATES COVERED (From - To)
	New Reprint	-

4. TITLE AND SUBTITLE
Metamorphic InAsSb/AlInAsSb heterostructures for optoelectronic applications

5a. CONTRACT NUMBER
W911NF-11-1-0109

5b. GRANT NUMBER

5c. PROGRAM ELEMENT NUMBER
611102

6. AUTHORS
Leon Shterengas, David Westerfeld, Wendy L. Sarney, Stefan P. Svensson, Gregory Belenky, Ding Wang, Youxi Lin, Dmitry Donetsky, Gela Kipshidze

5d. PROJECT NUMBER

5e. TASK NUMBER

5f. WORK UNIT NUMBER

7. PERFORMING ORGANIZATION NAMES AND ADDRESSES
Research Foundation of SUNY at Stony Brook U
Office of Sponsored Programs
W-5510 Melville Library
Stony Brook, NY 11794 -3362

8. PERFORMING ORGANIZATION REPORT NUMBER

9. SPONSORING/MONITORING AGENCY NAME(S) AND ADDRESS(ES)
U.S. Army Research Office
P.O. Box 12211
Research Triangle Park, NC 27709-2211

10. SPONSOR/MONITOR'S ACRONYM(S)
ARO

11. SPONSOR/MONITOR'S REPORT NUMBER(S)
57965-EL.6

12. DISTRIBUTION AVAILIBILITY STATEMENT
Approved for public release; distribution is unlimited.

13. SUPPLEMENTARY NOTES
The views, opinions and/or findings contained in this report are those of the author(s) and should not contrued as an official Department of the Army position, policy or decision, unless so designated by other documentation.

14. ABSTRACT
Metamorphic heterostructures containing bulk InAs1?xSbx layers and AlInAsSb barriers were grown on GaSb substrates. The lattice mismatch (up to 2.1%) between the GaSb substrates and the InAsSb layers was accommodated by the growth of GaInSb linearly graded buffers. The 1??m thick InAsSb0.44 layer with an absorption edge above 9??m exhibited an in-plane residual strain of about 0.08%. InAs1?xSbx structures with x?=?0.2 and x?=?0.44 operated as light emitting diodes at 80?K demonstrated output powers of 90??W and 8??W

15. SUBJECT TERMS
aluminium compounds, arsenic compounds, buffer layers, III-V semiconductors, indium compounds, lattice constants, light emitting diodes, semiconductor epitaxial layers, semiconductor growth

16. SECURITY CLASSIFICATION OF:			17. LIMITATION OF ABSTRACT	15. NUMBER OF PAGES	19a. NAME OF RESPONSIBLE PERSON
a. REPORT	b. ABSTRACT	c. THIS PAGE			Gregory Belenky
UU	UU	UU	UU		19b. TELEPHONE NUMBER: 631-632-8397

Report Title

Metamorphic InAsSb/AlInAsSb heterostructures for optoelectronic applications

ABSTRACT

Metamorphic heterostructures containing bulk InAs1?xSbx layers and AlInAsSb barriers were grown on GaSb substrates. The lattice mismatch (up to 2.1%) between the GaSb substrates and the InAsSb layers was accommodated by the growth of GaInSb linearly graded buffers. The 1??m thick InAsSb0.44 layer with an absorption edge above 9??m exhibited an in-plane residual strain of about 0.08%. InAs1?xSbx structures with x?=?0.2 and x?=?0.44 operated as light emitting diodes at 80?K demonstrated output powers of 90??W and 8??W at 5??m and 8??m, respectively.

REPORT DOCUMENTATION PAGE (SF298)
(Continuation Sheet)

Continuation for Block 13

ARO Report Number 57965.6-EL
Metamorphic InAsSb/AlInAsSb heterostructures ...

Block 13: Supplementary Note

Approved for public release; distribution is unlimited.

Metamorphic InAsSb/AlInAsSb heterostructures for optoelectronic applications

Gregory Belenky,[1] Ding Wang,[1] Youxi Lin,[1] Dmitry Donetsky,[1] Gela Kipshidze,[1] Leon Shterengas,[1] David Westerfeld,[1] Wendy L. Sarney,[2] and Stefan P. Svensson[2]
[1]*Department of ECE, Stony Brook University, New York 11794, USA*
[2]*U.S. Army Research Laboratory, 2800 Powder Mill Rd., Adelphi, Maryland 20783, USA*

(Received 21 January 2013; accepted 8 March 2013; published online 20 March 2013)

Metamorphic heterostructures containing bulk $InAs_{1-x}Sb_x$ layers and AlInAsSb barriers were grown on GaSb substrates. The lattice mismatch (up to 2.1%) between the GaSb substrates and the InAsSb layers was accommodated by the growth of GaInSb linearly graded buffers. The 1 μm thick $InAsSb_{0.44}$ layer with an absorption edge above 9 μm exhibited an in-plane residual strain of about 0.08%. $InAs_{1-x}Sb_x$ structures with $x = 0.2$ and $x = 0.44$ operated as light emitting diodes at 80 K demonstrated output powers of 90 μW and 8 μW at 5 μm and 8 μm, respectively. © *2013 American Institute of Physics*. [http://dx.doi.org/10.1063/1.4796181]

The development of highly efficient light emitting devices and detectors operating in the spectral region above 5 μm using III-V fabrication technology remains an important task. Infrared (IR) light emitting diodes (LEDs) have potential applications such as pollutant gas sensing, molecular spectroscopy, process monitoring, noninvasive disease analysis, and infrared scene projection.[1–3] IR photodetectors have broad applications in imaging and environmental and industrial monitoring.[4] Type-II superlattices (T2SLs) are a key structure used in IR devices designed for these technologies. However, not all IR device design requirements can be satisfied by using T2SLs. The short minority carrier lifetimes of $\tau < 100$ ns (Ref. 5) in InAs/Ga(In)Sb T2SLs are detrimental to the performance of photodetectors due to their effects on the dark current. InAs/$InAs_{1-x}Sb_x$ structures with interband optical transitions near 10 μm are characterized by longer minority lifetimes $\tau \sim 400$ ns,[6] but the growth of these structures requires the utilization of thick layers of InAs.[6,7] The latter suppresses the interband optical coefficient[7,8] and impedes hole transport along the growth direction. The hole transport limitation and the low value of the interband matrix element of the active layer affect the performance of LEDs and nBn type "barrier" detectors.

All these challenges can be overcome by using InAsSb bulk layers in the active regions of the device heterostructures. The bandgap of the InAsSb alloys can be tailored in a range from below 100 meV to above 300 meV by choosing the group V element content.[9,10] However the growth of an alloy with a fundamental absorption edge in the vicinity of 10 μm requires about 40% Sb composition and implies a lattice mismatch of about 2%–2.5% with respect to the GaSb or InSb substrate.

We have recently demonstrated that by using a compositionally graded buffer,[11] high quality InAsSb bulk layers can be grown on a virtual substrate with lattice constants up to 2.1% larger than that of GaSb. The structural, recombination, and optical characteristics of these layers were described in Ref. 12. This approach opens the opportunity of developing types of barrier optoelectronic devices for the spectral region near and above 5 μm. The active region of these emitters and detectors will be potentially free from the fundamental transport and optical transition limitations associated with InAs/$InAs_{1-x}Sb_x$ materials.

In this paper, we will discuss the characteristics of heterostructures containing bulk $InAs_{1-x}Sb_x$ and lattice matched AlInAsSb barriers. The structures were grown on graded InGaSb buffers on GaSb substrates. Devices with $InAs_{1-x}Sb_x$ layers having $x = 0.2$ and $x = 0.44$ operated in LED mode at 80 K demonstrated output powers up to 90 μW and 8 μW at 5 μm and 8 μm, respectively.

The structures were grown by solid-source molecular beam epitaxy in a Veeco Gen-930. The growth details were described in Ref. 13. The composition of the GaInSb buffer was linearly graded over 2 μm to $GaIn_{0.8}Sb_{0.2}$ or over 3 μm to $GaIn_{0.6}Sb_{0.4}$. Then 500 nm thick $Ga_{0.87}In_{0.13}Sb$ or $Ga_{0.64}In_{0.36}Sb$ virtual substrates were grown with their native lattice parameters matched to the in-plane lattice parameter of the top strained part of the buffer. Finally, the InAsSb/AlInAsSb/InAsSb heterostructure was grown on top lattice matched to the virtual substrate.

The lattice parameters of the individual layers in the metamorphic heterostructures were quantified by high resolution X-ray diffraction analysis. Figure 1 shows the reciprocal space maps (RSM) measured near the asymmetric (335) reflex of the GaSb substrate. The RSM measurements were performed at 0 and 180° azimuthal angles with respect to the [110] direction. The [110] and [-1-10] RSM data were averaged to compensate for the tilt of the metamorphic layers with respect to the GaSb substrate.[12] The line drawn through the reflex from the GaSb substrate corresponds to the (335) reflexes of an ideal, completely relaxed cubic lattice with an increasing lattice constant. It can be seen that the bottom portion of the compositionally graded buffer has cubic symmetry, i.e., it is nearly 100% relaxed, since the corresponding reflexes are grouped around the line drawn through the GaSb (335) reflex. The top part of the compositionally graded buffer is pseudomorphically strained and has a constant in-plane but an increasing out-of-plane lattice parameter. The active region heterostructure layers grown on top of the compositionally graded buffers produce peaks in RSM which are located near the intercept of the 100% relaxation and the vertical line corresponding to the top portion of the grade.

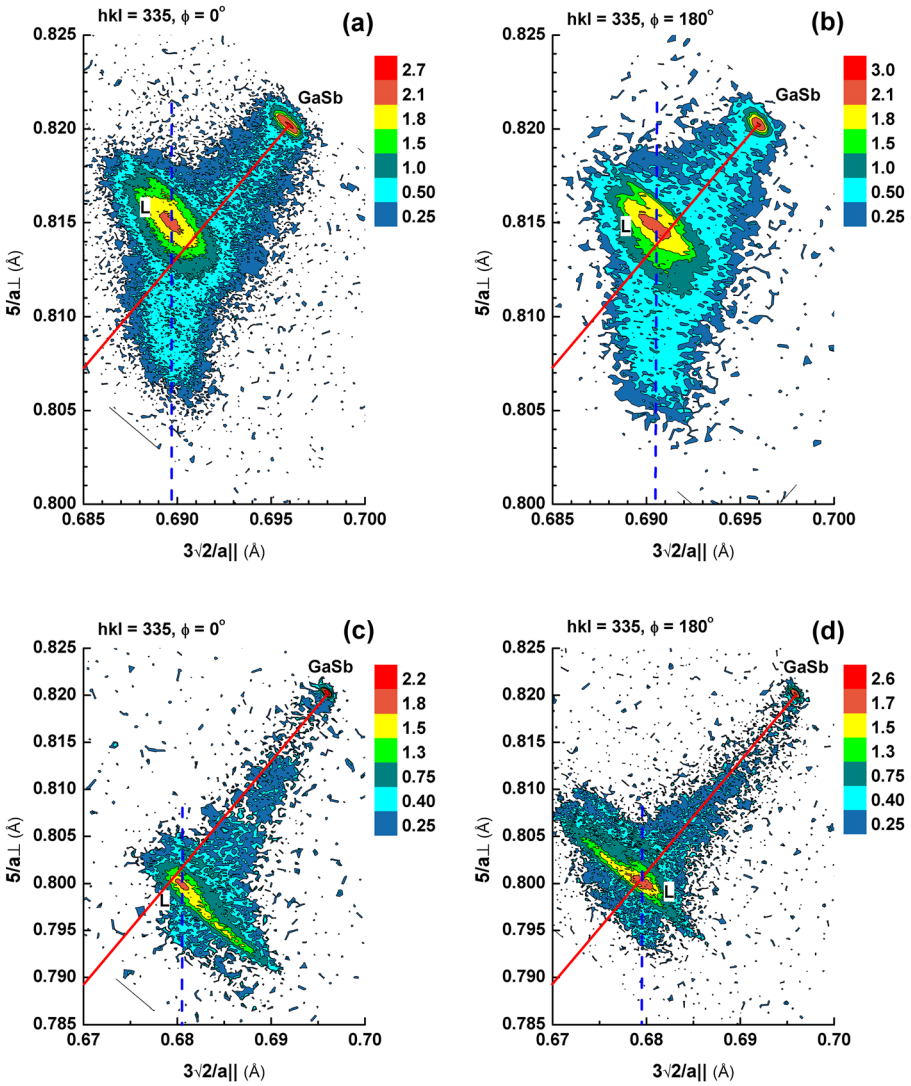

FIG. 1. Asymmetric (335) RSMs measured for structures with $InAs_{0.8}Sb_{0.2}$ (a),(b) and $InAs_{0.56}Sb_{0.44}$ (c),(d) in the [110] and [-1-10] directions. The reciprocal lattice point corresponding to the 1-μm-thick InAsSb layer is marked as L. The solid red line denotes the location of 335 reflexes of fully relaxed materials, and the vertical dashed blue line denotes that of the materials grown pseudomorphically on top of the buffer. Shown in the legend is the common logarithm of the x-ray intensity in the unit of counts/s.

Thus, we conclude that the heterostructure is nearly undistorted cubic and is grown pseudomorphically to the in-plane lattice parameter of the compositionally graded buffer layer. The amount of residual strain in the heterostructure was determined by direct measurement of the in-plane (100) and (010) and perpendicular (001) lattice parameters from the RSM data. Using a linear interpolation for the C_{11} and C_{12} elastic constants[14] and the standard relationship between strains in perpendicular directions ($\varepsilon = -2\frac{c_{12}}{c_{11}}\varepsilon_{||}$)[15] we determined the residual strains and composition of the $InAs_{1-x}Sb_x$ layers. The residual in-plane strain for the sample with the $InAs_{0.8}Sb_{0.2}$ layer is 0.09% while the sample with the $InAs_{0.56}Sb_{0.44}$ layer exhibited a residual in-plane strain of 0.08%. Low residual strain values imply no relaxation and thus no formation of misfit dislocations in the heterostructure layers. This is confirmed by RSM results showing that peaks from InAsSb are located on the same vertical line as the cloud of reflexes from the pseudomorphic part of the compositionally graded buffers.

To obtain information about electroluminescence characteristics, two different metamorphic InAsSb/AlInAsSb heterostructures were designed and grown on InGaSb buffers. The corresponding layer compositions, thicknesses, and doping profiles are presented in Table I. Figure 2 shows an example of the schematic band diagram for the LED structure with x = 0.2. The composition of the quaternary barrier layer was chosen to align the valence band to that of the InAsSb.

The wafers were processed into LEDs as follows. The epilayer side of all structures was covered with a 300 nm thick silicon nitride dielectric layer. Windows of 400 μm diameter were opened in the dielectric, and a top Ti/Pt/Au metal contact was deposited. The wafers were lapped down to about 200 μm; Ni/Au/Ge/Ni/Au was deposited on the n-GaSb substrate and annealed followed by Ti/Pt/Au n-side

TABLE I. List of the composition, thickness, and doping of each layer in the LED heterostructures. The virtual substrates, buffers, and GaSb substrates in all structures were Te-doped to a nominal dopant concentration of $1 \times 10^{18}\,cm^{-3}$.

$InAs_{1-x}Sb_x$	$Al_{1-y}In_yAs_{1-z}Sb_z$	$InAs_{1-x}Sb_x$ contact
	Composition thickness doping	
x = 0.2	y = 0.4, z = 0.71	x = 0.2
0.5 μm	200 nm	200 nm
Undoped	Be: $1 \times 10^{18}\,cm^{-3}$	Be: $1 \times 10^{19}\,cm^{-3}$
x = 0.44	y = 0.65, z = 0.72	x = 0.44
0.5 or 1 μm	200 nm	200 nm
Undoped	Be: $1 \times 10^{18}\,cm^{-3}$	Be: $1 \times 10^{19}\,cm^{-3}$

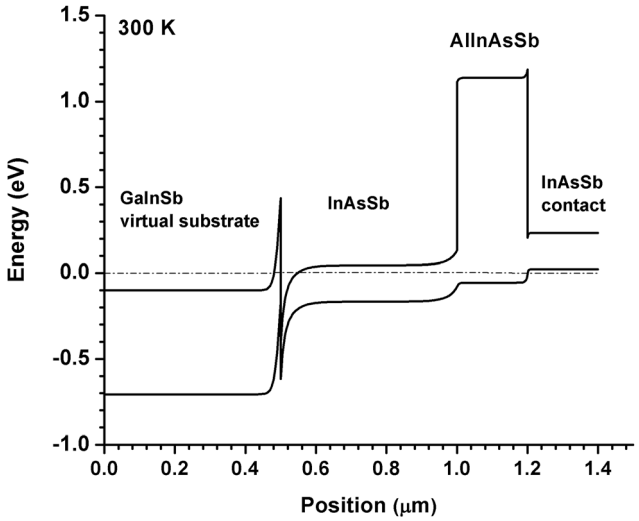

FIG. 2. Schematic band diagram for an LED with x = 0.2 at zero bias. It consists of a 500 nm nominally undoped $InAs_{0.8}Sb_{0.2}$ active layer, a 200 nm Be-doped (p: 1×10^{18} cm^{-3}) $Al_{0.6}In_{0.4}As_{0.29}Sb_{0.71}$ barrier, and a 200 nm heavily Be-doped (p: 1×10^{19} cm^{-3}) $InAs_{0.8}Sb_{0.2}$ contact layer. The dashed-dotted line denotes the Fermi level.

metallization. Electroluminescence was collected through 500 μm diameter windows in the n-side metallization. No antireflection coating was applied. The LEDs were cleaved into 600 μm × 600 μm squares.

Figure 3 shows the electroluminescence spectra and LED output power for structures with x = 0.2 (a),(b) and 0.44 (c),(d), respectively. The structure with x = 0.2 exhibited 90 μW total emitted power at a wavelength around 5 μm at 77 K and 10 μW at room temperature. The structure with x = 0.44 emitted 8 μW at 77 K at a peak wavelength of about 8 μm. The blue shift of the energy position of electroluminescence peak in Figure 3(c) (for x = 0.44, $E_g \leq 0.120$ eV (Ref. 10)) is explained by band filling under electrical injection.

The optical power was measured using calibrated indium-antimonide and mercury-cadmium-telluride photodetectors. All light emitted from the LED surface was coupled to one aperture of a gold-plated integrating sphere with a photodetector mounted in another aperture; thus, no assumptions about the LED's direction diagram had to be made. The photodetector-integrating-sphere setup was calibrated using a black-body source operated at 800 °C. The emission of the black-body was sent through an 8 mm diameter aperture and was measured using a calibrated thermopile photodetector and used for photodetector calibration. Spectra of the photodetector responsivity and LED electroluminescence were measured by Fourier transform and grating spectrometers.

The output power of the 8 μm LEDs with 0.5-μm-wide and 1-μm-wide InAsSb layers is shown in Figure 3(d). The external efficiency and output power of the LED with the 1-μm-thick active region was almost twice as high as the structures with the 0.5 μm thick active region. This implies that Shockley-Reed-Hall recombination does not control the device current. Data presented in Figure 3(d) are evidence of the fact that the hole diffusion length of the $InAs_{1-x}Sb_x$ layer is of μm scale which is advantageous for LED and photo detector development.

We demonstrated that the growth of GaInSb compositionally graded buffers allows the fabrication of heterostructures containing bulk InAsSb and AlInAsSb layers with lattice constants up to 2.1% larger than that of the GaSb substrate. The 1 μm thick $InAs_{0.56}Sb_{0.44}$ layer with an absorption edge above 9 μm (see Fig. 3(c)) is characterized by an in-plane residual strain of about 0.08%. The result opens the opportunity to develop heterostructures containing wide-gap barriers and thick (1–3 μm) narrow-gap III-V emitters/absorbers with bandgap energies much lower than that of InSb. These structures with a high interband optical

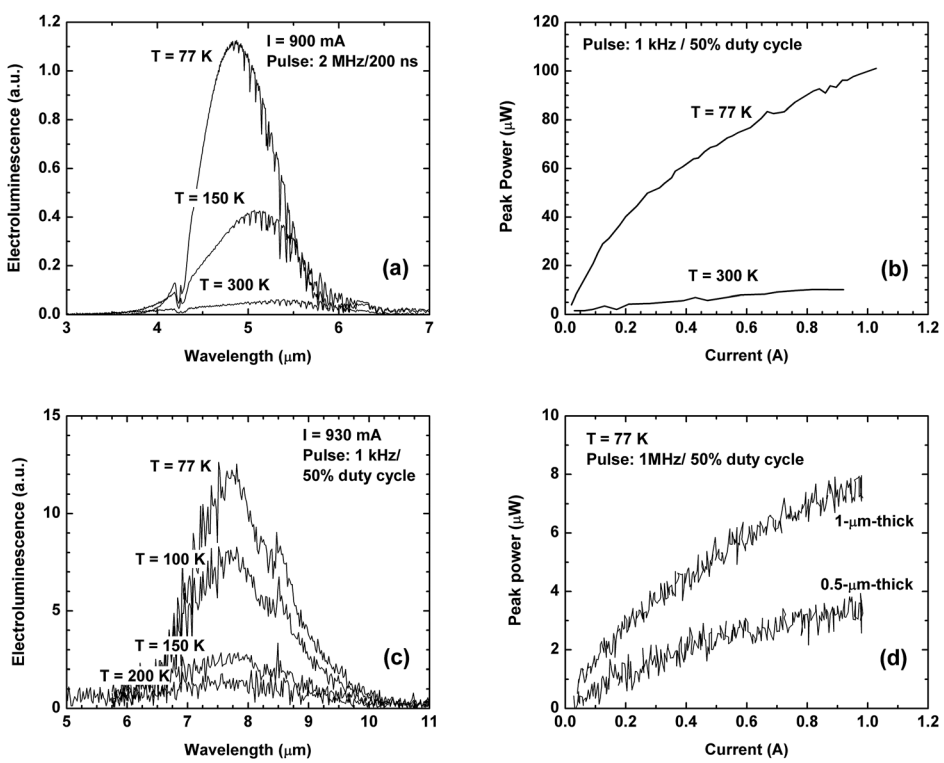

FIG. 3. Electroluminescence spectra and L-I curves for $InAs_{1-x}Sb_x$ LED with x = 0.2 (a),(b) and x = 0.44 (c),(d).

coefficient and excellent transport characteristics are suitable for the design of IR LEDs, nBn, and other types of barrier photodetectors. In the latter case the localization of the electric field exclusively in the barrier area can lead to significant dark current suppression.

This work was supported by US National Science Foundation through grant (No. DMR1160843) and US Army Research Office through grants (Nos. W911NF1110109 and W911NF1220057).

[1]J. G. Crowder, H. R. Hardaway, and C. T. Elliott, Meas. Sci. Technol. **13**, 882–884 (2002).
[2]N. V. Zotova, N. D. Il'inskaya, S. A. Karandashev, B. A. Matveev, M. A. Remennyi, and N. M. Stus', Semiconductors **40**, 697–703 (2006).
[3]E. J. Koerperick, D. T. Norton, J. T. Olesberg, B. V. Olson, J. P. Prineas, and T. F. Boggess, IEEE J. Quantum Electron. **47**, 50–54 (2011).
[4]See, e.g., A. Rogalski and K. Chrzanowski, Opto-Electron. Rev. **10**, 111–136 (2002), available at http://www.wat.edu.pl/review/optor/10(2)111.pdf.
[5]D. Donetsky, G. Belenky, S. P. Svensson, and S. Suchalkin, Appl. Phys. Lett. **97**, 052108 (2010).
[6]E. H. Steenbergen, B. C. Connelly, G. D. Metcalfe, H. Shen, M. Wraback, D. Lubyshev, Y. Qiu, J. M. Fastenau, A. W. K. Liu, S. Elhamri, O. O. Cellek, and Y.-H. Zhang, Appl. Phys. Lett. **99**, 251110 (2011).
[7]D. Lackner, M. Steger, M. L. W. Thewalt, O. J. Pitts, Y. T. Cherng, S. P. Watkins, E. Plis, and S. Krishna, J. Appl. Phys. **111**, 034507 (2012).
[8]E. H. Steenbergen, K. Nunna, L. Ouyang, B. Ullrich, D. L. Huffaker, D. J. Smith, and Y.-H. Zhang, J. Vac. Sci. Technol. B **30**, 02B107 (2012).
[9]A. Rogalski, *Infrared Detectors*, 2nd ed. (CRC, Boca Raton, 2011), p. 341.
[10]S. P. Svensson, W. L. Sarney, H. Hier, Y. Lin, D. Wang, D. Donetsky, L. Shterengas, G. Kipshidze, and G. Belenky, Phys. Rev. B **86**, 245205 (2012).
[11]G. Belenky, D. Donetsky, G. Kipshidze, D. Wang, L. Shterengas, W. L. Sarney, and S. P. Svensson, Appl. Phys. Lett. **99**, 141116 (2011).
[12]D. Wang, Y. Lin, D. Donetsky, L. Shterengas, G. Kipshidze, G. Belenky, W. L. Sarney, H. Hier, and S. P. Svensson, Proc. SPIE **8353**, 835312 (2012).
[13]G. Kipshidze, T. Hosoda, W. L. Sarney, L. Shterengas, and G. Belenky, IEEE Photon. Tech. Lett. **23**, 317–319 (2011).
[14]I. Vurgaftman, J. R. Meyer, and L. R. Ram-Mohan, J. Appl. Phys. **89**, 5815 (2001).
[15]U. Pietsch, V. Holy, and T. Baumbach, *High-Resolution X-Ray Scattering: from Thin Films to Lateral Nanostructures*, 2nd ed. (Springer, New York, 2004), p. 180.